Energy levels and structure of tetraatomic van der Waals clusters

Pablo Villarreal, Octavio Roncero, and Gerardo DelgadoBarrio

Citation: J. Chem. Phys. **101**, 2217 (1994); doi: 10.1063/1.467662
View online: http://dx.doi.org/10.1063/1.467662
View Table of Contents: http://jcp.aip.org/resource/1/JCPSA6/v101/i3
Published by the American Institute of Physics.

Energy levels and structure of tetra-atomic van der Waals clusters

Pablo Villarreal, Octavio Roncero, and Gerardo Delgado-Barrio
Instituto de Matemáticas y Física Fundamental, C.S.I.C., Serrano 123, 28006 Madrid, Spain

(Received 29 December 1993; accepted 4 April 1994)

A variational treatment is presented to study bound and quasibound states of $X_1\cdots BC\cdots X_2$ van der Waals clusters, where X_1 and X_2 are rare gas atoms and BC is a conventional diatomic molecule. The Hamiltonian operator, including all the degrees of freedom, is expressed in terms of the B–C relative vector and bond coordinates which describe the position of each rare gas atom with respect to the BC center of mass. In a body-fixed reference system, with the Z axis parallel to the diatomic axis, all the matrix elements of the Hamiltonian are evaluated in a basis set of functions which takes into account the symmetries of the system. Numerical applications to the $He_2\cdots Cl_2$ and $Ne_2\cdots I_2$ complexes are presented and discussed.

I. INTRODUCTION

Since the pioneering studies of Levy and co-workers on vibrational predissociation (VP) of clusters composed of iodine and several rare gas atoms,[1] a great deal of research effort has been devoted to this kind of complex. Using supersonic molecular beams to get extremely low temperatures it is possible through the application of optical laser spectroscopy to answer crucial points about the structure and VP dynamics of these clusters. In this way, Levy and co-workers determined, within the accuracy of the experiment, binding energies of the complexes, the dependence of the VP rate on the initial vibrational energy stored in the diatomic subunit, the role of additivity of interactions through the band-shift analysis as the size of the cluster increases, as well as the vibrational distribution of the diatomic fragment after dissociation. Furthermore, by incorporating a second delayed laser which excites the isolated diatomic product to an upper electronic state, and detecting its fluorescence in the case of lighter diatomic subunits than I_2, not only vibrational but also rotational distributions were determined, providing additional insight about the structure and dynamics of the systems under study. This technique was successfully applied to systems like $X_2\cdots Cl_2$, with X=He,[2] Ne,[3] and Ar[4] by Janda and co-workers, and to $Ne_n\cdots ICl$[5] by Lester and co-workers, for which the congestion in the rotational spectrum of the diatom is not so pronounced as for the case of iodine. Recently, by means of pump–probe/molecular beam methodology using pulses in the subpicosecond scale, real-time experiments for $Ne_n\cdots I_2$ ($n=2$–4) were conducted by Zewail and co-workers,[6] examining the pathways for direct VP and for the onset of intramolecular vibrational energy redistribution (IVR) as a function of the cluster size.

From the theoretical point of view, complexes of I_2 and two rare gas atoms were studied in the collinear configuration[7] by means of quasiclassical trajectories (QCT) and applying the classical limit of the time-dependent self-consistent-field (SCF) method. The goal was to elucidate the competition in the flowing of energy from the iodine to each weak bond. Also, assuming a coplanar configuration, QCT calculations[8(a)] as well as quantum ones[8(b)] based on the Fermi's Golden Rule were carried out.

For a nonrotating iodine molecule, and restricting the rare gas atoms to move along a plane perpendicular to the diatomic axis, some calculations were performed for a pure sequential model of fragmentation[9] by using an angular adiabatic plus Golden Rule approach. The branching ratio among this sequential pathway and the double continuum channel[10(a)] or the dissociation producing two diatomic fragments was also analyzed,[10(b)] predicting a dominance of the sequential mechanism. Using quantal distributions[11] to generate the initial conditions, QCT dynamical calculations were performed on $I_2\cdots X_n$ ($n=1$–9) clusters.[12] In this way, the relative importance of the different fragmentation channels and the incidence of IVR as a function of the number of rare gas atoms were examined, predicting a magic cluster size of $n=8$.

Recently, Gray and co-workers[13] carried out wave packet (WP) calculations for $X_2\cdots Cl_2$, X=He and Ne, vdW clusters. They considered a three degrees of freedom model closely related to the one already used,[9] obtaining not only a qualitative but, in some features, quantitative agreement with the available experimental data.[2,3] Regarding the relative importance of dissociation pathways, their calculations show that the sequential mechanism is operative in both cases, He and Ne, although for the latter the direct fragmentation mechanism is enhanced with decreasing the angle formed by the two weak bonds.

All the above dynamical calculations were performed within some kind of reduced dimension framework. Regarding the calculations of quasibound states required for dynamical as well as spectroscopic studies, several approaches have been reported in the literature. An approximate variational quantum treatment which includes all degrees of freedom for $J=0$ was proposed[11] to calculate the bound states of $I_2\cdots XY$ systems (X,Y=He,Ne). Such a model is based on a molecular orbital formalism, involving the approximations of neglecting the iodine rotation and those kinetic coupling terms in the Hamiltonian which are divided by the I_2 mass. Recently, Bačić *et al.*[14] reported exact quantum Monte Carlo calculations on the ground vdW state of $He_n\cdots Cl_2$ ($n=2,3$) complexes. Their results display the floppiness of the $He_2\cdots Cl_2$ molecule, in agreement with the analysis of the

 0021-9606/94/101(3)/2217/14/$6.00

experimental absorption spectrum,[2] and moreover, emphasize the importance of doing exact calculations for such liquid-like molecules. In this sense, and in order to properly interpret the rotationally resolved excitation spectrum of $He_2\cdots Cl_2$,[2] variational calculations involving nonzero total angular momenta including all the degrees of freedom have been recently carried out[15] by using a molecular orbital treatment.[11]

In this work, we present an alternative way to get not only the ground but also some accurate excited states of tetra-atomic $X_1\cdots BC\cdots X_2$ vdW clusters, providing the possibility of interpreting the experimental spectra. In addition, such states can be used to perform several types of dynamical studies of VP, such as QCT,[7,8(a),12,16,17] WP,[13] or hemiquantal[18] calculations. The coordinate system used[9–13,15–17] is expressed in terms of the BC intramolecular vector and bond coordinates to describe the position of the rare gas atoms with respect to the BC center of mass. These non-Jacobian coordinates involve an unusual kinetic coupling term in the Hamiltonian, but both the sequential and the double continuum fragmentation channels are then explicitly described in the dynamical calculations. The dissociation in two diatomic systems may be accounted for,[13] but when this mechanism becomes dominant it is more adequate to study the fragmentation dynamics using pure Jacobian coordinates as it has been done for diatomic–diatomic[19(a),19(b),19(d)] and for $Ar_2\cdots HCl$[19(c),19(e)] van der Waals complexes. However, in the VP dynamics of the systems under study, the sequential dissociation of the complex is dominant[1–4,12,13] and the non-Jacobian coordinates are more adapted.

In order to solve the vibro-rotational problem, we choose a body-fixed frame with the BC bond parallel to the Z axis in a similar way as in previous works using Jacobian coordinates.[19] By adopting a variational procedure, we define a basis set composed of products of numerically adapted vibrational functions and angular functions in which the rotations associated to the weak bonds are described in a coupled representation. No restrictions are imposed on the different motions within the cluster, and the Hamiltonian is fully described, including the kinetic coupling term, whatever the total angular momentum considered be. Moreover, the symmetry properties of the Hamiltonian (parity under inversion of all the particle coordinates, permutation in the $X_1\equiv X_2$, case and interchanging of B and C in the homonuclear situation) are discussed and used to redefine symmetry-adapted basis functions for the cases under study.

For a total angular momentum $J=0$, numerical calculations on $He_2\cdots Cl_2$ and $Ne_2\cdots I_2$ are performed. These complexes exhibit very different features. Due to the weakness of the interaction between the light He atoms, the $He_2\cdots Cl_2$ is quite delocalized with respect to He atom positions. In turn, the heavier Ne atoms interact more strongly, leading to a much more localized structure. $He_2\cdots Cl_2$ was chosen to serve as a test of the method by comparing with the previous calculations of Bačić *et al.*[14] In this case, the procedure leads one to deal with matrices of moderate sizes, and convergence is achieved by using standard diagonalization methods. On the contrary, the $Ne_2\cdots I_2$ system forced us to use prediagonalization techniques and/or recursive methods such as the Lanczos[20] method. The quasibound states obtained for this system are used to generate the necessary initial conditions to perform QCT calculations.[16,17]

The paper is organized as follows. The general formalism is described in Sec. II, while Sec. III is devoted to discussion of the numerical results. Finally, the conclusions of this work are summarized in Sec. V.

II. GENERAL FORMALISM

We consider a four-particle system composed of two rare gas atoms, X_1 and X_2, weakly bound to an ordinary BC diatomic molecule. In spite of its simplicity, it is worthwhile to develop the Hamiltonian for this system in terms of Jacobi coordinates for the diatomic partner and bond coordinates, which go from the BC center of mass (c.m.) to the respective X_1 and X_2 atoms.

A. The Hamiltonian

In the total center of mass (C.M.) reference system, the kinetic operator

$$T=-\frac{\hbar^2}{2}\left[\frac{1}{m_{X_1}}\nabla^2_{X_1}+\frac{1}{m_{X_2}}\nabla^2_{X_2}+\frac{1}{m_B}\nabla^2_B+\frac{1}{m_C}\nabla^2_C\right] \quad (1)$$

may be rewritten, after using the relative vector $\mathbf{r}=\mathbf{R}_B-\mathbf{R}_C$ and the vector $\mathbf{R}$ going from C.M. to c.m.,

$$\mathbf{R}_B=\frac{m_C}{m_B+m_C}\mathbf{r}+\mathbf{R},$$
$$\mathbf{R}_C=\frac{-m_B}{m_B+m_C}\mathbf{r}+\mathbf{R}, \quad (2)$$

as follows:

$$T=-\frac{\hbar^2}{2}\left[\frac{1}{m_{X_1}}\nabla^2_{X_1}+\frac{1}{m_{X_2}}\nabla^2_{X_2}+\frac{m_B+m_C}{m_Bm_C}\nabla^2_r+\frac{1}{m_B+m_C}\nabla^2_R\right]. \quad (3)$$

The vectors $\mathbf{R}_1$ and $\mathbf{R}_2$ going from the center of mass of BC to X_1 and X_2, respectively, are related to $\mathbf{R}_{X_1}$, $\mathbf{R}_{X_2}$, and $\mathbf{R}$ through

$$\mathbf{R}_{X_1}=\frac{1}{M}[(m_B+m_C+m_{X_2})\mathbf{R}_1-m_{X_2}\mathbf{R}_2],$$
$$\mathbf{R}_{X_2}=\frac{1}{M}[-m_{X_1}\mathbf{R}_1+(m_B+m_C+m_{X_1})\mathbf{R}_2], \quad (4)$$
$$\mathbf{R}=-\frac{1}{M}(m_{X_1}\mathbf{R}_1+m_{X_2}\mathbf{R}_2),$$

M being the total mass of the system. Now, the kinetic operator finally takes the form

$$T=-\hbar^2\left\{\frac{\nabla^2_r}{2\mu_{BC}}+\frac{\nabla^2_1}{2\mu_{X_1,BC}}+\frac{\nabla^2_2}{2\mu_{X_2,BC}}+\frac{\nabla_1\cdot\nabla_2}{m_B+m_C}\right\}, \quad (5)$$

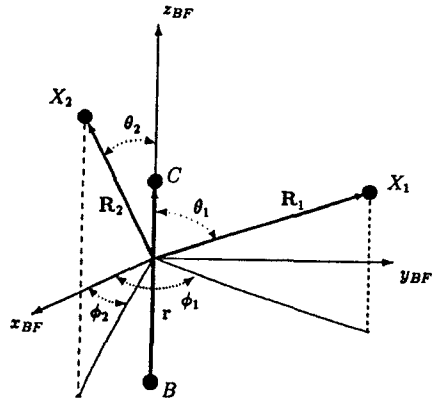

FIG. 1. Body-fixed coordinate system for a tetratomic $X_1\cdots BC\cdots X_2$ complex.

where we have introduced the corresponding reduced masses $\mu_{BC}=(m_B m_C)/(m_B+m_C)$ and $\mu_{X_i,BC} = m_{X_i}(m_B + m_C)/(m_{X_i} + m_B + m_C)$. The kinetic operator of Eq. (5) is analogous to that of a light–heavy–light three-particle system[21] in which the heavy atom is substituted by a diatomic molecule including its internal kinetic energy.

In addition, the total angular momentum with respect to C.M. is readily expressed as $\mathbf{J}=\mathbf{j}+\mathbf{l}_1+\mathbf{l}_2$ where $\mathbf{j}$ is the angular momentum of BC while $\mathbf{l}_i$ are the angular momenta associated to $\mathbf{R}_i$, $i=1$, 2 with respect to c.m.

Expressing now the ∇^2 operators in spherical coordinates (see Fig. 1), the Hamiltonian operator becomes

$$H=-\frac{\hbar^2}{2\mu_{BC}}\left(\frac{\partial^2}{\partial r^2}+\frac{2}{r}\frac{\partial}{\partial r}\right)+\frac{\mathbf{j}^2}{2\mu_{BC}r^2}-\frac{\hbar^2}{2\mu_{X_1,BC}}\left(\frac{\partial^2}{\partial R_1^2}+\frac{2}{R_1}\frac{\partial}{\partial R_1}\right)+\frac{\mathbf{l}_1^2}{2\mu_{X_1,BC}R_1^2}-\frac{\hbar^2}{2\mu_{X_2,BC}}\left(\frac{\partial^2}{\partial R_2^2}+\frac{2}{R_2}\frac{\partial}{\partial R_2}\right)+\frac{\mathbf{l}_2^2}{2\mu_{X_2,BC}R_2^2}-\frac{\hbar^2}{m_B+m_C}\nabla_1\cdot\nabla_2+V(\mathbf{r},\mathbf{R}_1,\mathbf{R}_2). \quad (6)$$

The potential V in Eq. (6) for these kind of systems is described by a sum of interactions as

$$V(\mathbf{r},\mathbf{R}_1,\mathbf{R}_2)=V_{BC}(r)+V_{X_1,BC}(r,R_1,\theta_1)+V_{X_2,BC}(r,R_2,\theta_2)+V_{X_1X_2}(|\mathbf{R}_1-\mathbf{R}_2|), \quad (7)$$

where $\cos\theta_i=\mathbf{R}_i\cdot\mathbf{r}/rR_i$.

B. The basis functions

In a body-fixed (BF) frame in which the Z axis always points in the $\hat{\mathbf{r}}$ direction, we consider basis functions composed of products of radial and angular functions,

$$\Phi^{JM}_{l_1l_2L\Omega vmn}(\mathbf{r},\mathbf{R}_1,\mathbf{R}_2)=\phi_{vmn}(r,R_1,R_2)\times\mathscr{W}^{JM}_{l_1l_2L\Omega}(\hat{\mathbf{r}},\hat{\mathbf{R}}_1,\hat{\mathbf{R}}_2). \quad (8)$$

The radial function ϕ is in turn a product:

$$\phi_{vmn}(r,R_1,R_2)=\frac{\chi_v(r)\xi^{(1)}_m(R_1)\xi^{(2)}_n(R_2)}{rR_1R_2}, \quad (9)$$

where $\chi_v(r)$ is an eigenfunction of the nonrotating isolated diatomic molecule,

$$\left[-\frac{\hbar^2}{2\mu_{BC}}\frac{\partial^2}{\partial r^2}+V_{BC}(r)\right]\chi_v(r)=E_{BC}(v)\chi_v(r) \quad (10)$$

and the $\xi^{(1)}(R_1),\xi^{(2)}(R_2)$ functions are also vibrational basis functions for the R_1,R_2 coordinates and will be specified later on.

The angular function $\mathscr{W}^{JM}_{l_1l_2L\Omega}(\hat{\mathbf{r}},\hat{\mathbf{R}}_1,\hat{\mathbf{R}}_2)$ depends on the diatomic orientation $\hat{\mathbf{r}}\equiv(\theta_r,\phi_r)$ with respect to a space-fixed (SF) frame, and on the orientations $\hat{\mathbf{R}}_i\equiv(\theta_i,\phi_i)$ with respect to the diatomic axis. These angular functions are written as[19,22]

$$\mathscr{W}^{JM}_{l_1l_2L\Omega}(\hat{\mathbf{r}},\hat{\mathbf{R}}_1,\hat{\mathbf{R}}_2)=\sqrt{\frac{2J+1}{4\pi}}D^{J*}_{M\Omega}(\phi_r,\theta_r,0)\mathscr{Y}^{L\Omega}_{l_1l_2}(\hat{\mathbf{R}}_1,\hat{\mathbf{R}}_2), \quad (11)$$

where $D^J_{M\Omega}$ constitute Wigner rotation matrices[23,24] relating the SF and BF frames corresponding to a total angular momentum J with projections M and Ω on the Z_{SF} and Z_{BF} axes, respectively. In Eq. (11), $\mathscr{Y}^{L\Omega}_{l_1l_2}$ are angular functions in the coupled representation referred to the body-fixed frame,[19(a)] which take the form

$$\mathscr{Y}^{L\Omega}_{l_1l_2}(\hat{\mathbf{R}}_1,\hat{\mathbf{R}}_2)=(-1)^{L+\Omega}\sqrt{2L+1}\sum_{\omega}\begin{pmatrix} l_1 & l_2 & L\\ -\omega & \omega-\Omega & \Omega\end{pmatrix}\times Y_{l_1\omega}(\theta_1,\phi_1)Y_{l_2\Omega-\omega}(\theta_2,\phi_2), \quad (12)$$

where $(\cdots)$ denotes $3-j$ symbols and $Y_{l_i\omega}(\theta_i,\phi_i)$ are spherical harmonics.

Total wave functions with well-defined values of J and M can be written as a linear combination of the basis functions of Eq. (8):

$$\Psi^{(JM)}_k=\sum_{l_1l_2L\Omega vmn}A^{l_1l_2L\Omega vmn}_k\Phi^{JM}_{l_1l_2L\Omega vmn} \quad (13)$$

with the coefficients $A^{l_1l_2L\Omega vmn}_k$ being obtained by solving the Schrödinger equation

$$H\Psi^{(JM)}_k=E_k\Psi^{(JM)}_k, \quad (14)$$

where E_k are the corresponding eigenvalues. Equation (14) is solved by representing the Hamiltonian in the basis set of Eq. (8) and diagonalizing the resulting matrix.

Besides its intrinsic interest, it is worthwhile to consider the symmetry of the Hamiltonian in Eq. (6) in order to reduce as much as possible the size of the matrix to be diagonalized. In addition to overall rotations, the Hamiltonian is invariant under inversion $\mathscr{E}^*$ of all the particles in the SF frame. In Appendix A we show that the angular basis functions of Eq. (11) transform as

$$\mathscr{E}^*[\mathscr{W}^{JM}_{l_1l_2L\Omega}(\hat{\mathbf{r}},\hat{\mathbf{R}}_1,\hat{\mathbf{R}}_2)] = (-1)^{J+l_1+l_2+L}\mathscr{W}^{JM}_{l_1l_2L-\Omega}(\hat{\mathbf{r}},\hat{\mathbf{R}}_1,\hat{\mathbf{R}}_2). \quad (15)$$

Thus, we consider the following linear combinations as the angular basis functions:

$$\mathscr{F}^{JMp=\pm1}_{l_1l_2L|\Omega|} = \sqrt{\frac{1}{2(1+\delta_{|\Omega|0})}}\,[\mathscr{W}^{JM}_{l_1l_2L|\Omega|} + p(-1)^{J+l_1+l_2+L}\,\mathscr{W}^{JM}_{l_1l_2L-|\Omega|}] \quad (16)$$

which are eigenfunctions of $\mathscr{E}^*$ with eigenvalue p. Therefore, the well-defined parity basis set becomes

$$\Phi^{JMp}_{l_1l_2L|\Omega|vmn}(\mathbf{r},\mathbf{R}_1,\mathbf{R}_2) = \phi_{vmn}(r,R_1,R_2)\mathscr{F}^{JMp}_{l_1l_2L|\Omega|}(\hat{\mathbf{r}},\hat{\mathbf{R}}_1,\hat{\mathbf{R}}_2). \quad (17)$$

If the two rare gas atoms are of the same species, $X_1 \equiv X_2$, the Hamiltonian is also invariant through their permutation $\mathscr{P}_{12}$ such that $\hat{\mathbf{R}}_1 \leftrightarrow \hat{\mathbf{R}}_2$. We obtain (see Appendix A)

$$\mathscr{P}_{12}[\Phi^{JMp}_{l_1l_2L|\Omega|vmn}] = (-1)^{l_1+l_2+L}\,\Phi^{JMp}_{l_2l_1L|\Omega|vnm}. \quad (18)$$

In this case the basis functions are built up as follows:

$$\Phi^{JMpp_{12}=\pm1}_{l_1l_2L|\Omega|vmn} = \sqrt{\frac{1}{2(1+\delta_{mn}\delta_{l_1l_2})}}\,[\Phi^{JMp}_{l_1l_2L|\Omega|vmn} + p_{12}(-1)^{l_1+l_2+L}\,\Phi^{JMp}_{l_2l_1L|\Omega|vnm}] \quad (19)$$

and are simultaneously eigenfunctions of $\mathscr{E}^*$, $\mathscr{P}_{12}$, and $\mathscr{P}^*_{12} = \mathscr{E}^* \times \mathscr{P}_{12}$.

In addition, when the diatomic subunit is homonuclear, i.e., B≡C, the wave function either remains unchanged or changes the sign, by the replacement $\hat{\mathbf{r}} \rightarrow -\hat{\mathbf{r}}$. Let $\mathscr{P}_{BC}$ be the corresponding operator. In Appendix A it is shown that

$$\mathscr{P}_{BC}[\mathscr{W}^{JM}_{l_1l_2L\Omega}] = (-1)^{J+L}\mathscr{W}^{JM}_{l_1l_2L-\Omega} \quad (20a)$$

so the parity functions $\mathscr{F}$ given in Eq. (16) satisfy that

$$\mathscr{P}_{BC}[\mathscr{F}^{JMp}_{l_1l_2L|\Omega|}] = p(-1)^{l_1+l_2}\mathscr{F}^{JMp}_{l_1l_2L|\Omega|}. \quad (20b)$$

All these symmetry properties of tetra-atomic systems correspond to those previously derived for similar basis functions but using different coordinates.[19]

C. Matrix elements

We now evaluate the matrix elements of the Hamiltonian using the basis functions of Eq. (8). For symmetry-adapted basis functions, Eq. (19), the corresponding matrix elements are then readily obtained from the previous ones.

The matrix elements of the $\mathbf{j}^2$ operator are obtained using the relation $\mathbf{j}=\mathbf{J}-\mathbf{L}$, with $\mathbf{L}=\mathbf{l}_1+\mathbf{l}_2$, and introducing raising and lowering operators[22]

$$\mathbf{J}_\pm = \mathbf{J}_x \pm i\mathbf{J}_y, \quad \mathbf{L}_\pm = \mathbf{L}_x \pm i\mathbf{L}_y.$$

In this way, one finds

$$\langle\mathscr{W}^{JM}_{l_1l_2L\Omega}|\mathbf{j}^2|\mathscr{W}^{JM}_{l_1'l_2'L'\Omega'}\rangle = \hbar^2\delta_{l_1l_1'}\delta_{l_2l_2'}\delta_{LL'}\{\delta_{\Omega\Omega'}[J(J+1)+L(L+1)-2\Omega^2] - \delta_{\Omega\Omega'\pm1}\sqrt{J(J+1)-\Omega\Omega'}\sqrt{L(L+1)-\Omega\Omega'}\}. \quad (21)$$

Therefore, $\mathbf{j}^2$ is diagonal in this representation with one exception: it also couples *tumbling* quantum numbers Ω and $\Omega\pm1$ as it is the case for triatomic systems.[22] For the diatomic rotational energy we get

$$\langle\Phi^{JM}_{l_1l_2L\Omega vmn}|\frac{\mathbf{j}^2}{2\mu_{BC}r^2}|\Phi^{JM}_{l_1'l_2'L'\Omega'v'm'n'}\rangle = \frac{\delta_{mm'}\delta_{nn'}}{2\mu_{BC}}\langle\mathscr{W}^{JM}_{l_1l_2L\Omega}|\mathbf{j}^2|\mathscr{W}^{JM}_{l_1'l_2'L'\Omega'}\rangle \times\int_0^{+\infty}dr\;\chi_v(r)r^{-2}\chi_{v'}(r). \quad (22)$$

On the other hand, the $\mathbf{l}_1^2$ operator is fully diagonal,[22] and the matrix elements of the *end-over-end* angular term are

$$\langle\Phi^{JM}_{l_1l_2L\Omega vmn}|\frac{\mathbf{l}_1^2}{2\mu_{X_1,BC}R_1^2}|\Phi^{JM}_{l_1l_2L\Omega v'm'n'}\rangle = \frac{\hbar^2l_1(l_1+1)}{2\mu_{X_1,BC}}\delta_{vv'}\delta_{nn'}\int_0^{+\infty}dR_1\;\xi^{(1)}_m(R_1)R_1^{-2}\xi^{(1)}_{m'}(R_1) \quad (23)$$

and a similar expression holds for $\mathbf{l}_2^2$.

With regard to the kinetic coupling term it is found that (see Appendix B)

$$\frac{-\hbar^2}{m_B+m_C}\langle\Phi^{JM}_{l_1l_2L\Omega vmn}|\nabla_1\cdot\nabla_2|\Phi^{JM}_{l_1'l_2'L'\Omega'v'm'n'}\rangle = \frac{-\hbar^2}{m_B+m_C}\delta_{vv'}\delta_{LL'}\delta_{\Omega\Omega'}(-1)^{L-l_1'+l_1} \times\begin{Bmatrix} l_2' & L & l_1' \\ l_1 & 1 & l_2\end{Bmatrix}G_1(m,m',l_1,l_1')G_2(n,n',l_2,l_2') \quad (24)$$

with $\{\cdots\}$ being $6-j$ symbols and

$$G_i(p,q,l,j) = \delta_{lj\pm1}(-1)^s\sqrt{s}\int_0^{+\infty}dR_i\;\xi^{(i)}_p(R_i) \times\left[\frac{d\xi^{(i)}_q(R_i)}{dR_i} \mp s\,\frac{\xi^{(i)}_q(R_i)}{R_i}\right], \quad (25)$$

where $s=\max(l,j)$. Note that this term is unable to change v, L, or Ω and only couples states with $l_1 = l_1' \pm 1$ and $l_2 = l_2' \pm 1$.

The $V_{X_i,BC}(r,R_i,\cos\theta_i)$ interactions are expanded in terms of Legendre polynomials as

$$V_{X_i,BC}(r,R_i,\cos\theta_i) = \sum_{\lambda_i} v_{\lambda_i}(r,R_i)P_{\lambda_i}(\cos\theta_i) \quad (26)$$

so that the matrix elements of, e.g., $V_{X_i,BC}$ are given by (see Appendix C)

$$\langle \Phi^{JM}_{l_1 l_2 L\Omega v m n} | V_{X_1,BC} | \Phi^{JM}_{l_1' l_2' L'\Omega' v' m' n'} \rangle$$
$$= \delta_{l_2 l_2'} \delta_{\Omega\Omega'} \delta_{nn'} (-1)^{\Omega - l_2}$$
$$\times \sqrt{(2L+1)(2L'+1)(2l_1+1)(2l_1'+1)}$$
$$\times \sum_{\lambda_1} v_{\lambda_1}^{vm;v'm'} \begin{Bmatrix} l_1 & L & l_2 \\ L' & l_1' & \lambda_1 \end{Bmatrix} \begin{pmatrix} L & \lambda_1 & L' \\ \Omega & 0 & -\Omega \end{pmatrix}$$
$$\times \begin{pmatrix} l_1' & \lambda_1 & l_1 \\ 0 & 0 & 0 \end{pmatrix} \tag{27}$$

and a similar expression holds for those of $V_{X_2,BC}$ by exchanging l_1, l_1', m, and m' by l_2, l_2', n, and n', respectively. The coefficients $v_{\lambda_1}^{vm;v'm'}$ in Eq. (27) are

$$v_{\lambda_i}^{vm;v'm'} = \int_0^{+\infty} \int_0^{+\infty} dr\, dR_i\, v_{\lambda_i}(r,R_i) \chi_v(r) \chi_{v'}(r) \xi_m^{(i)} \times (R_i) \xi_{m'}^{(i)}(R_i). \tag{28}$$

Also, by expanding the $V_{X,Y}$ interaction as

$$V_{X_1,X_2}(R_1,R_2,\cos\gamma) = \sum_{\Lambda} v_\Lambda(R_1,R_2) P_\Lambda(\cos\gamma) \tag{29}$$

(where $\cos\gamma = \mathbf{R}_1 \cdot \mathbf{R}_2 / R_1 R_2$) the corresponding matrix elements become (see Appendix C)

$$\langle \Phi^{JM}_{l_1 l_2 L\Omega v m n} | V_{X_1,X_2} | \Phi^{JM}_{l_1' l_2' L'\Omega' v' m' n'} \rangle$$
$$= \delta_{vv'} \delta_{LL'} \delta_{\Omega\Omega'} (-1)^{l_1 - l_1' + L}$$
$$\times \sqrt{(2l_1+1)(2l_1'+1)(2l_2+1)(2l_2'+1)}$$
$$\times \sum_{\Lambda} v_\Lambda^{mn;m'n'} \begin{Bmatrix} l_1 & \Lambda & l_1' \\ l_2' & L & l_2 \end{Bmatrix} \begin{pmatrix} l_1 & \Lambda & l_1' \\ 0 & 0 & 0 \end{pmatrix}$$
$$\times \begin{pmatrix} l_2 & \Lambda & l_2' \\ 0 & 0 & 0 \end{pmatrix}, \tag{30}$$

where

$$v_\Lambda^{mn;m'n'} = \int_0^{\infty} \int_0^{\infty} dR_1\, dR_2\, v_\Lambda(R_1,R_2) \xi_m^{(1)}(R_1) \xi_{m'}^{(1)}(R_1) \times \xi_n^{(2)}(R_2) \xi_{n'}^{(2)}(R_2). \tag{31}$$

D. Distributions

Dealing with wave functions depending on so many degrees of freedom, it is interesting, in order to get physical insight, to analyze their dependence on only one variable, which involves getting first-order density matrices. For variables on which the wave function explicitly depends, such as R_i, $i=1$, 2, the corresponding distributions are easily obtained as

$$D(X) = \int d\tau |\Psi_k^{(JM)}(\tau)|^2 \delta(R_i - X), \tag{32}$$

where $d\tau$ is the volume element.

Angular distributions are estimated easier by assuming an expansion in Legendre polynomials, in such a way that for $\alpha = \theta_1, \theta_2, \gamma$,

$$D(\cos\alpha) = \sum_n d_n P_n(\cos\alpha), \tag{33}$$

where the d_n coefficients are obtained from

$$\langle \Psi_k^{(JM)} | P_n(\cos\alpha) | \Psi_k^{(JM)} \rangle = \frac{2}{2n+1} d_n \tag{34}$$

and these averages are analytically calculated from the potential matrix elements discussed above.

It is also interesting to get the distribution of $\rho = |\mathbf{R}_1 - \mathbf{R}_2|$. Since the wave functions do not explicitly depend on ρ, it is easier to first obtain the third-order density matrix $D^{(3)}(\cos\gamma, R_1, R_2)$ by using Eq. (34) at fixed values of R_1 and R_2. Then, using the relation

$$\cos\gamma = \frac{R_1^2 + R_2^2 - \rho^2}{2R_1R_2}$$

the distribution of ρ takes the form

$$D(\rho) = \int\int dR_1\, dR_2 \frac{\rho}{R_1 R_2} D^{(3)}(\cos\gamma, R_1, R_2), \tag{35}$$

where the $\rho/(R_1R_2)$ factor comes from the Jacobian of the transformation of coordinates, $(R_1, R_2, \gamma) \rightarrow (R_1, R_2, \rho)$.

III. RESULTS AND DISCUSSION

In this work, we study two systems: $He_2 \cdots Cl_2$ and $Ne_2 \cdots I_2$. For the two complexes there are experimental data available[1,2] which give information of the structure as well as about the VP dynamics. The study of their bound and quasibound levels is then important not only because they can serve to interpret structural data but also because these states are required to carry out dynamical calculations. Moreover, as the interactions between the rare gas atoms in the two complexes are quite different, they show different behavior as will be discussed.

We focus our attention on the ground and first excited vdW states of these complexes and, in order to describe these $X_2 \cdots B_2$ systems, we choose functions with eigenvalues $p = (-1)^{J+L+l_1+l_2}$, $p_{12} = (-1)^{l_1+l_2+L} = +1$ and $p_{BC} = p$ of the $\mathscr{E}^*$, $\mathscr{P}_{12}$, and $\mathscr{P}_{BC}$ symmetry operators defined above. Then, in the angular basis set required for the calculation only even values of L contribute. In addition, we consider the case $J=0$, for which L is equivalent to the rotational quantum number of the B_2 diatomic subunit. The calculation for higher J values can also be performed by resorting to the use of prediagonalization techniques.

With respect to the radial basis set of Eq. (9), we assume here the diabatic approach for the vibrational motion of the diatomic subunit, which has been applied succesfully for triatomic systems.[25] In order to reduce the Hamiltonian matrix size, it is important to carefully choose the $\xi_m^{(i)}$ radial functions describing the vibrational motions on R_1 and R_2. One possible choice would be to evaluate them as discrete solutions of the triatomic Schrödinger equation at a fixed orientation θ_i,

$$\left[-\frac{\hbar^2}{2\mu_{X_i,B_2}}\frac{\partial^2}{\partial R_i^2}+\langle\chi_v(r)|V_{X_i,B_2}(r,R_i,\theta_i)|\chi_v(r)\rangle\right.$$
$$\left.-E_m^{(i)}(\theta_i)\right]\xi_m^{(i)}(R_i;\theta_i)=0, \quad (36)$$

e.g., the equilibrium geometry that corresponds, for the systems studied here, to $\theta_i=\pi/2$. However, the basis obtained in this way is limited since only a few bound states are supported by the respective potentials. In addition, this basis should describe well vdW stretching excitations but it may fail in the description of angular excitations. Hence, we resort to divide the interval $[0,\pi/2]$ in a number of points (25 in this case), solve Eq. (26) at each configuration (only for the ground level in the present calculations), and then orthonormalize these functions through a Schmidt procedure.[26] These numerical functions are well adapted and only a few of them were required to achieve convergency for the ground and also some rotationally excited states of the systems studied here. For high excited van der Waals states the size of the numerical basis should be increased and then a discrete variable representation method[27] can result more efficient.[20(e)] The derivatives of the radial numerical functions, present in some of the terms of the Hamiltonian in Eq. (6), are evaluated by using the fast Fourier transform method[28] which has proved to be very efficient and accurate.

The expansions in terms of Legendre polynomials of the interaction potentials in Eqs. (26) and (29) were carried out by using Gauss–Legendre quadratures.[29] In order to expand $V_{X_1X_2}$ there are some technical difficulties when $R_1=R_2$, since the potential reaches infinity as γ goes to zero. However, that region is physically forbidden at the energies studied here, the maximun number of Legendre polynomials required in the calculations being limited by the angular basis set to $2l_i^{\max}$, where $l_i^{\max}$ is the maximum value of l_1 and l_2 needed to achieve convergence.

A. $He_2\cdots Cl_2$ system

For the $Ne_2\cdots Cl_2$ complex it was possible to simulate the spectrum assuming the structure of a tetrahedron.[3] Of course, the assumption of a rigid structure does not mean that these van der Waals molecules are rigid, since the interaction between the partners is weak. This approach is adequate as long as the energy difference between adjacent van der Waals levels is much larger than the rotational constants associated with the overall rotation. However, $He_2\cdots Cl_2$ has been found to be very floppy and models based on frozen geometries do not reproduce the experimental absorption spectrum.[2] This fact was already discussed in detail for $He_2\cdots I_2$[11] for which the distribution of $\phi_1-\phi_2$ at fixed values of R_1 and R_2 was much broader and delocalized than the corresponding $Ne_2\cdots I_2$ distribution because the He···He interaction is much weaker than that of Ne···Ne. The calculations on the complexes $X_2\cdots I_2$ were performed assuming that the iodine molecule does not rotate, which is a good approximation for these systems since I_2 is very heavy. However, for the case of complexes containing Cl_2 this approach can fail, since it is lighter. Recently Bačić *et al.* performed quantum Monte Carlo calculations[14] for the ground vdW level of $He_2\cdots Cl_2$ and found that the distance between the two He atoms varies in a large range, which constitutes again clear evidence of its floppiness. The potential model used in Ref. 14 is given by Eq. (7) where $V_{Cl_2}(r)$ and V_{HeHe} are described by Morse functions and $V_{He_iCl_2}$ by a sum of Morse functions depending on the two He···Cl distances. In this work we use the same potential surface.[14]

TABLE I. Energy levels of $He_2\cdots Cl_2$ referred to the $Cl_2(v=0, j=0)$ diatomic energy.

α	Exact	Without the $\nabla_1\cdot\nabla_2$ term
0	−18.553	−18.548
1	−17.285	−17.268
2	−13.891	−13.914
3	−9.734	−9.646
4	−8.624	−8.800
5	−8.095	−8.081
6	−6.028	−6.029
7	−5.748	−5.727
8	−4.150	−4.036
9	−2.293	−2.409

In the variational calculations presented here, only the $v=0$ vibrational level of Cl_2 was included and convergence was achieved using $l_1^{\max}=l_2^{\max}=12$, $L^{\max}=12$, and $m^{\max}=n^{\max}=4$, leading to a Hamiltonian matrix of order 2716×2716. This calculation spent 31 minutes of CPU time on an IBM RISC/6000-350. The energies of the first ten levels are listed in Table I, with respect to the diatomic energy of Cl_2 (B, $v=0$, $j=0$). Adding the diatomic energy of the chlorine subunit (-3016.764 cm^{-1}), the energy of the ground vdW level becomes -3035.32 cm^{-1}, very close to the GFMC value of -3035.55 cm^{-1} of Ref. 14. The energies of the first ten levels calculated excluding the kinetic coupling term are also shown in Table I. It is clearly seen that the effect of this term increases with the excitation since the l_i angular momenta of the He atoms also increase. As the van der Waals potential surfaces for the X and B electronic states of Cl_2 are not very different, the photon absorption cannot populate very high excited van der Waals levels. Therefore, the kinetic coupling term will not have a strong influence on the absorption spectrum. However, in dynamical studies this term can become important since large excitations of l_i may be reached.

In Fig. 2 the distributions of L and l_i ($i=1,2$) are presented for the first two levels ($\alpha=0$ and 1). It is found that for these two levels the distribution in L is the same while the distributions for l_i are very different showing that the first excitation corresponds to that of the angular motion of the two He atoms. The radial and angular distributions are shown in Figs. 3(a) and 3(b) for $\alpha=0$, 1. Those of R_i and $\cos\theta_i$ are the same for these two van der Waals levels. They show peaks at $R_i\approx 3.8$ Å and $\theta=\pi/2$, respectively, but show an important spreading around these values. However, the distributions of ρ and $\cos\gamma$, which describe the relative mo-

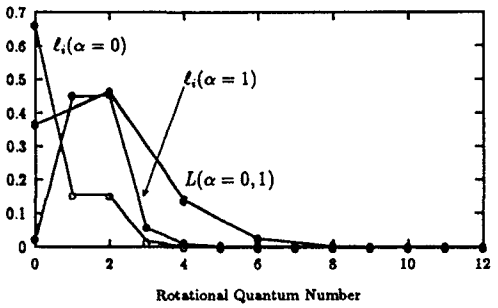

FIG. 2. Decomposition of the first two van der Waals levels (α=0,1) of $He_2\cdots Cl_2$ (v=0) in terms of the angular basis functions.

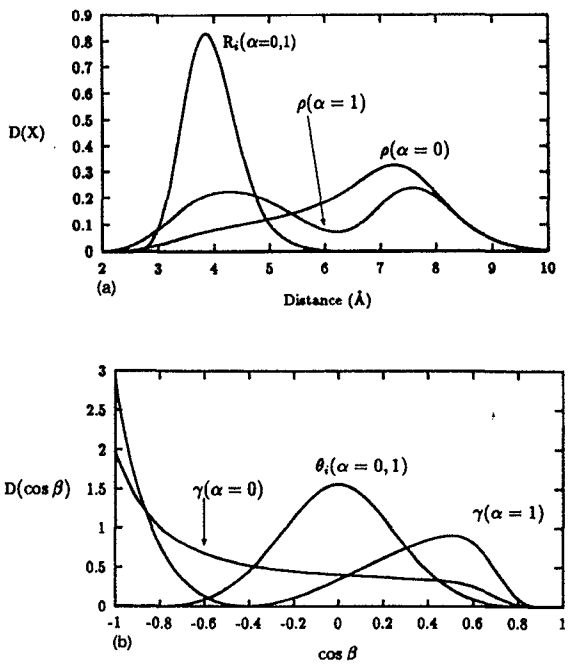

FIG. 3. Radial (a) and angular (b) distributions for the first two van der Waals levels of $He_2\cdots Cl_2$.

tion of the two He atoms, are much broader and different for α=0 and 1.

The distribution of ρ for the ground level is very similar to those obtained by Bačić[14] and shows a maximum at $\rho\approx$7.5 Å which corresponds to approximately twice the R_i equilibrium distance of each He to the center of mass of the Cl_2 subunit. The configuration at the maximum of all of these distributions corresponds to an almost planar structure with the helium atoms on opposite sides of the Cl–Cl bond. However, a well-defined equilibrium configuration does not exist since all the angular motions have very large amplitudes and practically all the angular region is available for the He atoms.

The ρ distribution for the first excited vdW level shows two maxima. The first one coincides with the shoulder of the ρ distribution for the ground state. The second peak corresponds to the planar structure already mentioned. Regarding the distributions of cos γ in Fig. 3(b) these features are also displayed. The distribution for the ground state is closely isotropic, except at the forbidden region around γ=0 where the two atoms collide.

Although all the $He_2\cdots Cl_2$ distributions are very broad, that corresponding to the He···He distance is the broadest, consistent with a simple model in which the two He atoms move keeping constant their distances to the center of mass of the diatomic subunit and on a plane perpendicular to the Cl_2 which is frozen.

Then, the Hamiltonian of Eq. (6) becomes

$$-\frac{\hbar^2}{2\mu_{X_1,BC}(R_1^{eq})^2}\frac{\partial^2}{\partial\phi_1^2}-\frac{\hbar^2}{2\mu_{X_2,BC}(R_2^{eq})^2}\frac{\partial^2}{\partial\phi_2^2}$$
$$+V_{HeHe}[\cos(\phi_1-\phi_2)]. \tag{37}$$

Due to the dependence of the potential on ϕ_1 and ϕ_2, we consider the following coordinates:

$$\phi_-=\phi_1-\phi_2,$$
$$\phi_+=(\phi_1+\phi_2)/2$$

such that the Hamiltonian of Eq. (37) takes the form

$$-\frac{\hbar^2}{4\mu_{X,BC}(R^{eq})^2}\frac{\partial^2}{\partial\phi_+^2}-\frac{\hbar^2}{\mu_{X,BC}(R^{eq})^2}\frac{\partial^2}{\partial\phi_-^2}+V_{HeHe}(\phi_-), \tag{38}$$

where R^{eq} is the distance of each He atom to the center of mass of Cl_2 at the maximum of the R_i distribution. In Eq. (38), the term depending on ϕ_+ describes the free rotation of the two heliums as a whole, while the remaining terms correspond to their relative motion. Then the associated eigenfunctions are written as

$$e^{i\Omega\phi_+}\Psi(\phi_-). \tag{39}$$

Here, the quantum number Ω is analogous to that in the three-dimensional treatment and only takes integer values. As $V_{HeHe}(\phi_-)=V_{HeHe}(-\phi_-)$, which corresponds to the permutation of the two He atoms, only even or odd Ψ solutions appear. Since we are considering $p_{12}=+1$, we expand $\Psi(\phi_-)$ in terms of even functions, for instance, $\{\cos n\phi_-\}_{n\in N}$. The energy differences between the ground and first excited van der Waals levels for the exact and model calculations agree fairly well, the values being 1.28 and 1.21 cm^{-1}, respectively. In Fig. 4 the square of the first two even eigenfunctions $\Psi^+(\phi_-)$ are shown together with the interaction potential. It is clearly seen that the two eigenfunctions are not restricted to the region of the potential well as their corresponding eigenvalues are positive (E_0^+=0.028 cm^{-1}). In addition, there is a nice qualitative agreement when the ϕ_- probabilities are compared with the distributions of γ for the first two van der Waals "exact" levels.

This model could be generalized to $J\neq0$ within an helicity decoupling scheme in which Ω becomes a good quantum number because it is not able to couple different Ω values as long as the rotation of BC is not considered. For $J\neq0$ a more appropriate reduced dimension model would be freezing all the radial coordinates (r, R_1, and R_2) at their equilibrium values and only solve for the angular motions.

B. $Ne_2\cdots I_2$ system

For this system there are previous calculations of bound states[11] where it was assumed that the iodine molecule does not rotate, which it is a good approximation since I_2 is very heavy. In this work we make use of the complete treatment presented above, where the assumption made in Ref. 11 is relaxed, and the only approach is to consider a vibrational diabatic scheme for the BC subunit.

The potential surface is based on atom–atom interactions described by Morse functions with parameters listed in Table II. The parameters for the Ne···I interaction were fitted[30] to reproduce the experimental lifetimes of $Ne\cdots I_2$.[31]

As was already discussed in Ref. 11, the angular as well as the radial motion amplitudes in $Ne_2\cdots I_2$ are narrower than for $He_2\cdots Cl_2$. This fact implies the use of a larger number of angular functions than for $He_2\cdots Cl_2$ but fewer radial functions. For the ground vdW level convergence up to 0.01 cm^{-1} was achieved using a basis set with $l_1^{max}=l_2^{max}=28$, $L=28$, and $m^{max}=n^{max}=2$. The resulting Hamiltonian matrix is of the order of 7000×7000 and is difficult to diagonalize by conventional methods. The procedure used consists of, first, getting an estimation of the eigenfunctions (which usually gives quite a good description) by diagonalizing a reduced Hamiltonian matrix (typically of the order of 3000×3000). In this case, this first diagonalization includes all the basis functions of Eq. (8) up to the limiting values $l_1=l_2=16$, $L=16$, and $m=n=2$. In a second step, we make use of the iterative Lanczos technique[20] with larger basis sets. In this method, the Lanczos algorithm is used to generate a subspace of eigenfunctions of the Hamiltonian in a recursive way from a particular initial guess. The Hamiltonian represented in this subspace is a tridiagonal matrix which is easily diagonalized by standard numerical techniques.[28] The ground-state function obtained is then used again to generate a new subspace, and this procedure is continued until the residue (overlap between the wave functions before and after each diagonalization) is smaller than a given criterium. In Fig. 5 we show how both the residue and the energy converge as a function of the iteration.

The energy of the ground vdW level for $v=17$ is -147.20 cm^{-1} and is about one wave number lower than the corresponding simple addition of $2D_0(Ne\cdots I_2)+D_0(Ne\cdots Ne)=-146.16$ cm^{-1}, suggesting that the Ne···Ne interaction is mixing $Ne\cdots I_2$ triatomic levels in the tetra-atomic system. The first excited level appears at -133.52 cm^{-1}, which is close to $2D_0(Ne\cdots I_2)$ plus the first Ne···Ne excitation of ≈-1.88 cm^{-1}. Hence, as in the $He_2\cdots Cl_2$ system, the first excitation corresponds to that of the Ne–Ne relative motion.

The probabilities for each value of L and l_i of the vdW ground state are presented in Fig. 6 and are much broader than those of $He_2\cdots Cl_2$. In particular, the distribution of l_i clearly indicates that the distributions of the ϕ_i angles are less isotropic than for $He_2\cdots Cl_2$, and this fact can be viewed in the distribution of $\cos\gamma$ shown in Fig. 7(a) which is located at $\gamma\approx\pi/4$. Also, the distribution of $\cos\theta_i$ in Fig. 7(a) is narrower than that of $He_2\cdots Cl_2$ and is located around $\pi/2$. The radial distribution of R_i is narrower than the corresponding to ρ, see Fig. 7(b), since the $Ne\cdots I_2$ interaction is stronger than the Ne···Ne one. All of these distributions are very localized which explains why the experimental absorption spectra can be well reproduced assuming a rigid tetrahedric structure for complexes containing two Ne atoms.[3]

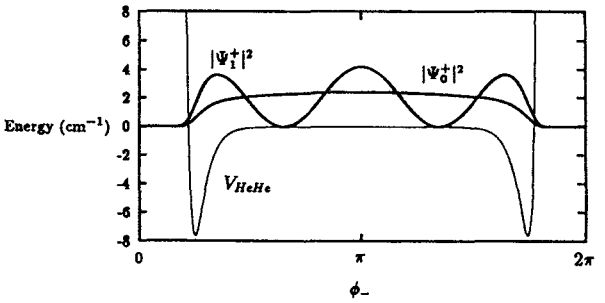

FIG. 4. Square of the first two levels obtained using the simple model of Eq. (38), in arbitrary units. The He–He interaction potential (in cm^{-1}) is also plotted.

The simple, reduced dimension model used for $He_2\cdots Cl_2$ can more properly be applied to $Ne_2\cdots I_2$. Thus, the first two levels calculated, Ψ_0^+ and Ψ_1^+, at -17.00 and -2.57 cm^{-1}, respectively, compare very nicely with the energies of free Ne_2 which are -16.56 and -1.88 cm^{-1}. The energies corresponding to the Ne···Ne motion in $Ne_2\cdots I_2$ are lower than those of free Ne_2, in agreement with the complete treatment. In Fig. 8 the square of Ψ_α^+ ($\alpha=0,1$) are presented. They confirm that the relative angular motion of the two Ne atoms is constrained to a small region which is completely different to the $He_2\cdots Cl_2$ case. The equilibrium value for the first level corresponds to $\phi_-=\pi/4$ which is consistent with the equilibrium value of the γ distribution in Fig. 7(a). This model explains in a very simple way the different behavior found between the two complexes studied here.

IV. CONCLUSIONS

In this work we have presented a full quantal treatment to obtain bound states of van der Waals clusters of the type $X_1\cdots BC\cdots X_2$. Local coordinates have been chosen to describe the relative motions of the rare gas atoms with respect to the center of mass of BC. In a body-fixed frame in which the Z axis lies parallel to the BC internuclear bond all the symmetries are taken into account. Furthermore, the matrix elements of the kinetic coupling term, appearing when using local coordinates, are explicitly given. The potential surface is approximated by a sum of atom–atom pairwise interactions which is very accurate to describe complexes with He

TABLE II. Potential parameters for the $Ne_2\cdots I_2$ system.

	R_e (Å)	D (cm^{-1})	α ($Å^{-1}$)
I···I[a]	3.027	5245.793	1.6832
Ne···I[b]	4.36	42.0	1.6
Ne···Ne[c]	3.091	29.36	2.088

[a]P. Luc, J. Mol. Spectrosc. **80**, 41 (1980).
[b]From Ref. 23.
[c]R. A. Aziz and M. J. Slaman, Chem. Phys. **130**, 187 (1989).

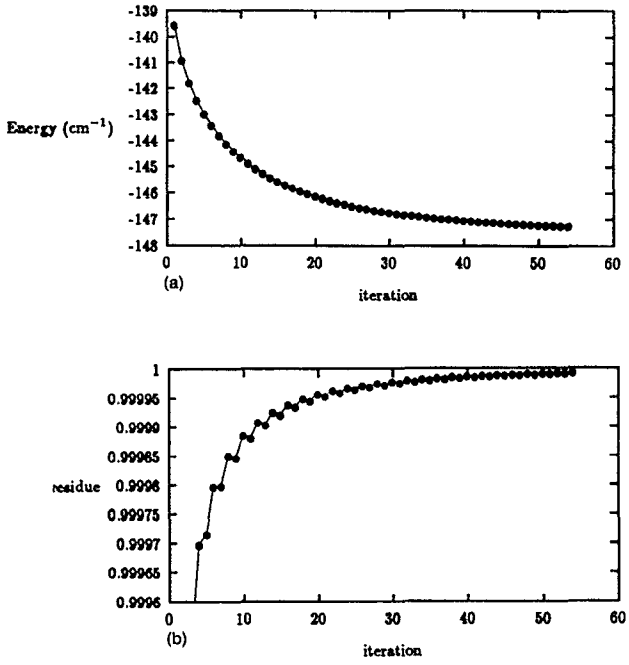

FIG. 5. Convergency analysis of the Lanczos procedure for the (a) ground level energy and (b) residue (see the text) as functions of the number of iterations applied to $Ne_2\cdots I_2$ ($v=17$).

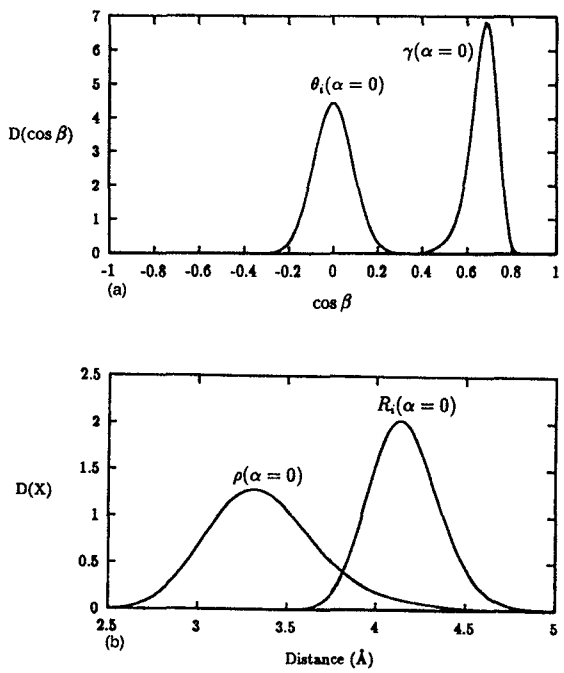

FIG. 7. Angular (a) and radial (b) distributions for the ground van der Waals level of $Ne_2\cdots I_2$ ($v=17$).

and/or Ne since these atoms are very slightly polarized and three-body terms may be neglected. For complexes containing Ar atoms some three-body terms have been reported (e.g., for $Ar_2\cdots HCl$ in Ref. 19) and they can be incorporated.

The present treatment has been applied to the study of $He_2\cdots Cl_2$ and $Ne_2\cdots I_2$ for $J=0$, calculating the ground as well as some excited van der Waals levels. It has been found that the two systems studied show different behavior. For the case of $Ne_2\cdots I_2$, the frequencies associated with the van der Waals modes are larger than the overall rotational constants of the complex, which explains why the experimental absorption spectra are well reproduced assuming a structure of a tetrahedron for these kind of systems.[3] However, in $He_2\cdots Cl_2$ the relative motion of the two He atoms is almost free and its associated frequency is of the order of the rotational constants of the whole system. This is the reason why the experimental absorption spectra for such systems[2] cannot be reproduced by models based on a frozen structure.

A simple model, in which the diatomic subunit motions are frozen and the two rare gas atoms move in a plane perpendicular to the BC intermolecular axis, is presented and used to make a comparative study of the two systems. It is found that the different behaviors are very nicely reproduced.

The energies and distributions obtained through the formalism presented here can be used to generate initial conditions for QCT calculations on the VP dynamics of these complexes. This procedure is now being applied to $Ne_2\cdots I_2$.[16,17]

A complete quantum approach for the dynamics is still far from being possible since there are too many degrees of freedom. However, restricted geometries can be assumed to perform dynamical calculations on VP of $Ne_2\cdots I_2$, as has done for $Ne\cdots I_2\cdots He$[9] and $Ne_2\cdots Cl_2$.[13]

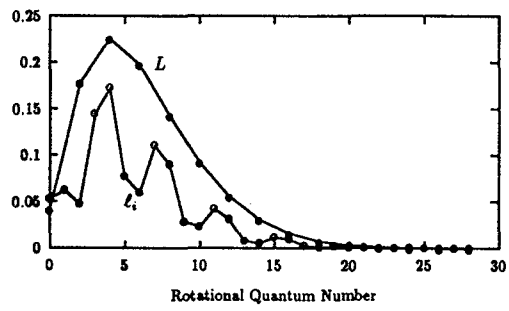

FIG. 6. Decomposition of the ground van der Waals level of $Ne_2\cdots I_2$ ($v=17$) in terms of the angular basis functions.

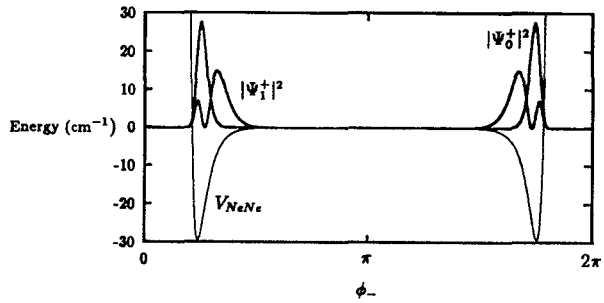

FIG. 8. Square of the first two levels obtained using the simple model of Eq. (38), in arbitrary units. The Ne–Ne interaction potential (in cm^{-1}) is also plotted.

ACKNOWLEDGMENTS

We thank M. Hernandez and N. Halberstadt for interesting discussions and for providing us results prior to publication. Also we want to thank A. García-Vela for his comments on the manuscript. Work was supported by DGICYT Grant No. PB92-0053, Comunidad Autónoma de Madrid Grant No. 064/92, and EEC Grant No. SC1.145.C.

APPENDIX A: APPLICATION OF SYMMETRY OPERATIONS

1. $\mathscr{E}^*$

We start by analyzing the result of applying the total inversion $\mathscr{E}^*$ operation on the basis functions of Eq. (8). Of course, unit vectors in SF transform as follows:[23]

$$\mathscr{E}^*:\hat{\mathbf{r}}\equiv(\theta_r,\phi_r)\rightarrow-\hat{\mathbf{r}}\equiv(\pi-\theta_r,\phi_r+\pi).$$

Now, to analyze how the original basis functions are transformed under this operation, we also have to determine the transformation of BF vectors, $\hat{\mathbf{R}}_1$ and $\hat{\mathbf{R}}_2$. Let us denote by $\hat{\mathbf{R}}$ one of these vectors, with polar angles (θ,ϕ) and (ϑ,φ) in the BF and SF frames, respectively. The spherical components $R_\nu,\nu=0,\pm1$, are proportional to spherical harmonics $Y_{1\nu}$, and under the rotation from the body-fixed to the space-fixed reference systems they transform as

$$Y_{1\nu}(\theta,\phi)=\sum_\mu D^1_{\mu\nu}(\phi_r,\theta_r,0)Y_{1\mu}(\vartheta,\varphi).$$

Therefore,

$$\mathscr{E}^*[Y_{1\nu}(\theta,\phi)]=\sum_\mu D^1_{\mu\nu}(\phi_r+\pi,\pi-\theta_r,0)\times Y_{1\mu}(\pi-\vartheta,\varphi+\pi).$$

Using the relationship between spherical harmonics and Wigner functions and their symmetry properties,[23] we obtain

$$\mathscr{E}^*[Y_{1\nu}(\theta,\phi)]=Y_{1\nu}(\theta,\pi-\phi),$$

i.e., under inversion, BF vectors transform as[22]

$$\mathscr{E}^*:\hat{\mathbf{R}}\equiv(\theta,\phi)\rightarrow\hat{\mathbf{R}}'\equiv(\theta,\pi-\phi).$$

Now we are in position to determine the effect of the inversion of all the four particles on the angular basis functions

$$\mathscr{E}^*[\mathscr{W}^{JM}_{l_1l_2L\Omega}]=\sqrt{\frac{2J+1}{4\pi}}D^{J*}_{M\Omega}(\phi_r+\pi,\pi-\theta_r,0)\times\mathscr{Y}^{L\Omega}_{l_1l_2}(\theta_1,\pi-\phi_1,\theta_2,\pi-\phi_2).$$

Using the relations

$$D^{J*}_{M\Omega}(\phi_r+\pi,\pi-\theta_r,0)=(-1)^JD^{J*}_{M-\Omega}(\phi_r,\theta_r,0),$$

$$\mathscr{Y}^{L\Omega}_{l_1l_2}(\theta_1,\pi-\phi_1,\theta_2,\pi-\phi_2)=(-1)^{l_1+l_2+L}\mathscr{Y}^{L-\Omega}_{l_1l_2}(\theta_1,\phi_1,\theta_2,\phi_2),$$

we finally get

$$\mathscr{E}^*[\mathscr{W}^{JM}_{l_1l_2L\Omega}]=(-1)^{J+l_1+l_2+L}\mathscr{W}^{JM}_{l_1l_2L-\Omega}.$$

2. $\mathscr{P}_{12}$

In the $X_1\equiv X_2$ case, the permutation operator $\mathscr{P}_{12}$ acts on the basis functions of Eq. (8) as follows:

$$\mathscr{P}_{12}[\Phi^{JM}_{l_1l_2L\Omega vmn}(\mathbf{r},\mathbf{R}_1,\mathbf{R}_2)]=\phi_{vmn}(r,R_2,R_1)\mathscr{W}^{JM}_{l_1l_2L\Omega}(\hat{\mathbf{r}},\hat{\mathbf{R}}_2,\hat{\mathbf{R}}_1)]$$

with

$$\phi_{vmn}(r,R_2,R_1)=\phi_{vnm}(r,R_1,R_2).$$

For the angular part, using Eqs. (11) and (12) we obtain

$$\mathscr{Y}^{L\Omega}_{l_1l_2}(\hat{\mathbf{R}}_2,\hat{\mathbf{R}}_1)=(-1)^{l_1-l_2+\Omega}\sqrt{2L+1}\sum_\omega\begin{pmatrix}l_1 & l_2 & L\\ \omega & \Omega-\omega & -\Omega\end{pmatrix}Y_{l_1\omega}(\theta_2,\phi_2)Y_{l_2\Omega-\omega}(\theta_1,\phi_1)$$

$$=(-1)^{l_1+l_2+L}(-1)^{l_1-l_2+\Omega}\sqrt{2L+1}\sum_{\omega'}\begin{pmatrix}l_2 & l_1 & L\\ \omega' & \Omega-\omega' & -\Omega\end{pmatrix}Y_{l_1\Omega-\omega'}(\theta_2,\phi_2)Y_{l_2\omega'}(\theta_1,\phi_1),$$

where $\omega'=\Omega-\omega$. Then

$$\mathscr{P}_{12}[\Phi^{JM}_{l_1l_2L\Omega vmn}(\mathbf{r},\mathbf{R}_1,\mathbf{R}_2)]=(-1)^{l_1+l_2+L}\Phi^{JM}_{l_2l_1L\Omega vnm}(\mathbf{r},\mathbf{R}_1,\mathbf{R}_2).$$

Note that this kind of relation holds if we replace the angular functions $\mathscr{W}$ by the parity functions $\mathscr{F}$ defined in Eq. (16).

3. $\mathscr{P}_{BC}$

Finally, if BC is homonuclear and we denote by $\mathscr{P}_{BC}$ the operator replacing $\hat{\mathbf{r}}$ by $-\hat{\mathbf{r}}$, i.e., it transforms the different angles as follows:

$$(\theta_r,\phi_r)\rightarrow(\pi-\theta_r,\phi_r+\pi),$$

$$(\theta_i,\phi_i)\rightarrow(\pi-\theta_i,-\phi_i),\quad i=1,2$$

we have

$$\mathscr{P}_{\mathrm{BC}}[\mathscr{Y}^{JM}_{l_1 l_2 L\Omega}] = \sqrt{\frac{2J+1}{4\pi}}\, D^{J*}_{M\Omega}(\phi_r+\pi, \pi-\theta_r, 0) \times \mathscr{Y}^{L\Omega}_{l_1 l_2}(\pi-\theta_1, -\phi_1, \pi-\theta_2, -\varphi_2).$$

Using the relations[23]

$$Y_{lm}(\pi-\theta,-\phi) = (-1)^l Y_{l-m}(\theta,\phi),$$

$$D^{J*}_{M\Omega}(\phi_r+\pi,\pi-\theta_r,0) = (-1)^J D^{J*}_{M-\Omega}(\phi_r,\theta_r,0),$$

we finally get

$$\mathscr{P}_{\mathrm{BC}}[\mathscr{Y}^{JM}_{l_1 l_2 L\Omega}] = (-1)^{J+L}\mathscr{Y}^{JM}_{l_1 l_2 L-\Omega}.$$

APPENDIX B: KINETIC COUPLING TERM MATRIX ELEMENTS

Once the gradient operators are expressed in terms of tensorial components

$$\nabla^{(i)}_0 = \partial/\partial z_i; \quad \nabla^{(i)}_{\pm 1} = \mp(\partial/\partial x_i \pm i\,\partial/\partial y_i)/\sqrt{2},$$

where the index $i=1,2$ is associated with the $\mathbf{R}_1$ and $\mathbf{R}_2$ vectors, the kinetic coupling term takes the form

$$\frac{-\hbar^2}{m_B+m_C}\nabla_1\cdot\nabla_2 = \frac{-\hbar^2}{m_B+m_C}\sum_{\nu=-1}^{1}(-1)^\nu \nabla^{(1)}_\nu \nabla^{(2)}_{-\nu}. \tag{B1}$$

Using the Wigner–Eckart theorem[24]

$$\left\langle Y_{l\omega}\frac{f(R)}{R}\middle|\nabla^{(i)}_\nu\middle|\frac{g(R)}{R}Y_{l'\omega'}\right\rangle = (-1)^{-\omega}\left[\begin{pmatrix} l & 1 & l' \\ -\omega & \nu & \omega' \end{pmatrix}\Big/\begin{pmatrix} l & 1 & l' \\ 0 & 0 & 0 \end{pmatrix}\right] \times \left\langle Y_{l0}\frac{f(R)}{R}\middle|\nabla^{(i)}_0\middle|\frac{g(R)}{R}Y_{l'0}\right\rangle$$

the matrix elements of the operator in Eq. (B1) between the functions of Eq. (8) become

$$\sum_{\nu=-1}^{1}(-1)^\nu\langle\Phi^{JM}_{l_1 l_2 L\Omega v m n}|\nabla^{(1)}_\nu\nabla^{(2)}_{-\nu}|\Phi^{JM}_{l_1' l_2' L'\Omega' v' m' n'}\rangle$$

$$= \delta_{\Omega\Omega'}\delta_{vv'}(-1)^{L+L'}\sqrt{(2L+1)(2L'+1)}\sum_{\nu\omega\omega'}(-1)^\nu\begin{pmatrix} l_1 & l_2 & L \\ -\omega & \omega-\Omega & \Omega \end{pmatrix}\begin{pmatrix} l_1' & l_2' & L' \\ -\omega' & \omega'-\Omega & \Omega \end{pmatrix}$$

$$\times\left\langle Y_{l_1 0}(\hat{\mathbf{R}}_1)\frac{\xi_m(R_1)}{R_1}\middle|\nabla^{(1)}_0\middle|\frac{\xi_{m'}(R_1)}{R_1}Y_{l_1'0}(\hat{\mathbf{R}}_1)\right\rangle\left\langle Y_{l_2 0}(\hat{\mathbf{R}}_2)\frac{\xi_n(R_2)}{R_2}\middle|\nabla^{(2)}_0\middle|\frac{\xi_{n'}(R_2)}{R_2}Y_{l_2'0}(\hat{\mathbf{R}}_2)\right\rangle$$

$$\times(-1)^{-\omega}\left[\begin{pmatrix} l_1 & 1 & l_1' \\ -\omega & \nu & \omega' \end{pmatrix}\Big/\begin{pmatrix} l_1 & 1 & l_1' \\ 0 & 0 & 0 \end{pmatrix}\right](-1)^{\omega-\Omega}\left[\begin{pmatrix} l_2 & 1 & l_2' \\ \omega-\Omega & -\nu & \Omega-\omega' \end{pmatrix}\Big/\begin{pmatrix} l_2 & 1 & l_2' \\ 0 & 0 & 0 \end{pmatrix}\right]. \tag{B2}$$

The task now is to calculate the matrix elements of ∇_0 appearing in the preceding equation. This operator is

$$\nabla_0 = \partial/\partial z = \cos\theta\,\partial/\partial R - (1/R)\sin\theta\,\partial/\partial\theta.$$

After some algebra we obtain

$$\cos\theta\, Y_{l'\omega'}(\theta,\phi) = \sqrt{\frac{(l'-\omega'+1)(l'+\omega'+1)}{(2l'+3)(2l'+1)}} \times Y_{l'+1\omega'}(\theta,\phi) + \sqrt{\frac{(l'+\omega')(l'-\omega')}{(2l'+1)(2l'-1)}}\, Y_{l'-1\omega'}(\theta,\phi)$$

and

$$\sin\theta\frac{\partial}{\partial\theta}Y_{l'\omega'}(\theta,\phi) = l'\sqrt{\frac{(l'-\omega'+1)(l'+\omega'+1)}{(2l'+3)(2l'+1)}}\, Y_{l'+1\omega'}(\theta,\phi) - (l'+1)\sqrt{\frac{(l'+\omega')(l'-\omega')}{(2l'+1)(2l'-1)}}\, Y_{l'-1\omega'}(\theta,\phi),$$

where the spherical harmonics have been expressed in terms of Legendre functions, and for the latter we have used[24]

$$(1-x^2)\frac{d}{dx}P^m_l(x) = (l+m)P^m_{l-1} - lxP^m_l(x).$$

Therefore, matrix elements of ∇_0 become

$$\left\langle\frac{f(R)}{R}Y_{l0}\middle|\nabla_0\middle|\frac{g(R)}{R}Y_{l'0}\right\rangle = \delta_{ll'\pm1}[(2l+1)(2l'+1)]^{-1/2}s \times\int_0^\infty dR\, f(R)\left[\frac{dg(R)}{dR}\mp s\frac{g(R)}{R}\right], \tag{B3}$$

where $s=\max(l,l')$.

Substituting Eq. (B3) in Eq. (B2) and using the explicit value of $\begin{pmatrix} l & 1 & l' \\ 0 & 0 & 0 \end{pmatrix}$ one finds

$$\sum_{\nu=-1}^{1}(-1)^{\nu}\langle\Phi^{JM}_{l_1l_2L\Omega\upsilon mn}|\nabla^{(1)}_{\nu}\nabla^{(2)}_{-\nu}|\Phi^{JM}_{l_1'l_2'L'\Omega'\upsilon'm'n'}\rangle$$

$$=\left[\sum_{\nu\omega\omega'}(-1)^{\nu-\Omega}\begin{pmatrix} l_1 & l_2 & L\\ -\omega & \omega-\Omega & \Omega\end{pmatrix}\begin{pmatrix} l_1' & l_2' & L'\\ -\omega' & \omega'-\Omega & \Omega\end{pmatrix}\begin{pmatrix} l_1 & 1 & l_1'\\ -\omega & \nu & \omega'\end{pmatrix}\begin{pmatrix} l_2 & 1 & l_2'\\ \omega-\Omega & -\nu & \Omega-\omega'\end{pmatrix}\right]\delta_{\Omega\Omega'}\delta_{\upsilon\upsilon'}$$

$$\times(-1)^{L+L'}\sqrt{(2L+1)(2L'+1)}G_1(m,m',l_1,l_1')G_2(n,n',l_2,l_2'),\tag{B4}$$

where the G_i, $i=1,2$ functions have been already defined, see Eq. (25).

The term within brackets in Eq. (B4) may be further simplified by using[23]

$$\sum_{\nu\omega t}(-1)^{\nu-\Omega}\begin{pmatrix} l_1 & l_2 & L\\ -\omega & \omega-\Omega & \Omega\end{pmatrix}\begin{pmatrix} l_2 & 1 & l_2'\\ \omega-\Omega & -\nu & -t\end{pmatrix}\begin{pmatrix} l_2' & L' & l_1'\\ t & \Omega & -t-\Omega\end{pmatrix}\begin{pmatrix} l_1 & 1 & l_1'\\ -\omega & \nu & t+\Omega\end{pmatrix}$$

$$=\sum_{\nu\omega t}(-1)^{\nu-\Omega}\begin{pmatrix} l_1 & l_2 & L\\ -\omega & \omega-\Omega & \Omega\end{pmatrix}\begin{pmatrix} l_2 & 1 & l_2'\\ \omega-\Omega & -\nu & -t\end{pmatrix}\sum_{K}(2K+1)(-1)^{l_2'+L'-l_1'+l_1+1+K+\nu+\Omega}\begin{Bmatrix} l_2' & L' & l_1'\\ l_1 & 1 & K\end{Bmatrix}$$

$$\times\begin{pmatrix} 1 & l_2' & K\\ \nu & t & \Omega-\omega\end{pmatrix}\begin{pmatrix} L' & l_1 & K\\ \Omega & -\omega & \omega-\Omega\end{pmatrix}.$$

Considering the orthogonality relationship of the 3-j symbols the bracked term in Eq. (B4) symplifies leading to Eq. (24).

APPENDIX C: MATRIX ELEMENTS OF POTENTIAL TERMS

1. $V_{X_i,BC}$

Concerning triatomic interactions, e.g., $V_{X_i,BC}$, by considering its expansion in Legendre polynomials, Eq. (26), which in turn can be expressed as spherical harmonics, and by using the integral[23]

$$\langle Y_{j_3m_3}|Y_{j_2m_2}|Y_{j_1m_1}\rangle=(-1)^{m_3}\sqrt{\frac{(2j_1+1)(2j_2+1)(2j_3+1)}{4\pi}}\begin{pmatrix} j_1 & j_2 & j_3\\ m_1 & m_2 & -m_3\end{pmatrix}\begin{pmatrix} j_1 & j_2 & j_3\\ 0 & 0 & 0\end{pmatrix},\tag{C1}$$

we have

$$\langle\Phi^{JM}_{l_1l_2L\Omega\upsilon mn}|V_{X_1,BC}(r,R_1,\cos\theta_1)|\Phi^{JM}_{l_1'l_2'L'\Omega'\upsilon'm'n'}$$

$$=\delta_{nn'}\delta_{\Omega\Omega'}\delta_{l_2l_2'}(-1)^{l_1+l_1'}\sqrt{(2L+1)(2L'+1)(2\ell_1+1)(2\ell_1'+1)}$$

$$\times\sum_{\lambda_1}v_{\lambda_1}^{\upsilon m;\upsilon'm'}\begin{pmatrix} l_1' & \lambda_1 & l_1\\ 0 & 0 & 0\end{pmatrix}\sum_{\omega}(-1)^{\omega}\begin{pmatrix} l_1 & l_2 & L\\ \omega & \Omega-\omega & -\Omega\end{pmatrix}\begin{pmatrix} l_1' & l_2' & L'\\ \omega & \Omega-\omega & -\Omega\end{pmatrix}\begin{pmatrix} l_1' & \lambda_1 & l_1\\ \omega & 0 & -\omega\end{pmatrix}\tag{C2}$$

where the $v_{\lambda_1}^{\upsilon m;\upsilon'm'}$ coefficients are radial integrals, see Eq. (28).

Using[23]

$$\begin{pmatrix} l_1 & L & l_2\\ -\omega & \Omega & \omega-\Omega\end{pmatrix}\begin{pmatrix} L' & l_1' & l_2\\ -\Omega & \omega & \Omega-\omega\end{pmatrix}$$

$$=\sum_{K}(2K+1)(-1)^{l_1+L-l_2+L'+l_1'+K+\omega+\Omega}\begin{Bmatrix} l_1 & L & l_2\\ L' & l_1' & K\end{Bmatrix}\begin{pmatrix} l_1' & l_1 & K\\ \omega & -\omega & 0\end{pmatrix}\begin{pmatrix} L & L' & K\\ \Omega & -\Omega & 0\end{pmatrix}$$

and accounting for the orthogonality relation

$$\sum_{\omega}\begin{pmatrix} l_1' & \lambda_1 & l_1\\ \omega & 0 & -\omega\end{pmatrix}\begin{pmatrix} l_1' & l_1 & K\\ \omega & -\omega & 0\end{pmatrix}=\delta_{K\lambda_1}(-1)^{l_1'+\lambda_1+l_1}(2\lambda_1+1)^{-1},$$

we finally arrive at Eq. (27) from Eq. (C2). The matrix elements of the $V_{X_2,BC}$ are obtained in a similar way.

2. V_{X_1,X_2}

Starting from the expansion in terms of Legendre polynomials, Eq. (29), and using the *spherical harmonic addition theorem*[23]

$$P_\Lambda(\cos\gamma)=\frac{4\pi}{2\Lambda+1}\sum_q Y^*_{\Lambda q}(\theta_1,\phi_1)Y_{\Lambda q}(\theta_2,\phi_2),$$

and the integral over three spherical harmonics, Eq. (C1), we have

$$\langle\Phi^{JM}_{l_1l_2L\Omega v mn}|V_{X_1,X_2}(R_1,R_2,\cos\gamma)|\Phi^{JM}_{l_1'l_2'L'\Omega' v' m' n'}\rangle$$

$$=\delta_{vv'}\delta_{\Omega\Omega'}(-1)^{l_1+l_1'-l_2-l_2'}\sqrt{(2L+1)(2L'+1)(2l_1+1)(2l_1'+1)(2l_2+1)(2l_2'+1)}\sum_\Lambda v_\Lambda^{mn;m'n'}\begin{pmatrix}l_1&\Lambda&l_1'\\0&0&0\end{pmatrix}$$

$$\times\begin{pmatrix}l_2&\Lambda&l_2'\\0&0&0\end{pmatrix}\sum_{q\omega\omega'}(-1)^{\omega'+\Omega-\omega}\begin{pmatrix}l_1&l_2&L\\\omega&\Omega-\omega&-\Omega\end{pmatrix}\begin{pmatrix}l_2'&\Lambda&l_2\\\Omega-\omega'&q&\omega-\Omega\end{pmatrix}\begin{pmatrix}l_1'&l_2'&L'\\\omega'&\Omega-\omega'&-\Omega\end{pmatrix}\begin{pmatrix}l_1&\Lambda&l_1'\\\omega&q&-\omega'\end{pmatrix}. \tag{C3}$$

Using once more the relation[23]

$$\begin{pmatrix}l_1&\Lambda&l_1'\\\omega&q&-\omega'\end{pmatrix}\begin{pmatrix}l_2'&L'&l_1'\\\Omega-\omega'&-\Omega&\omega'\end{pmatrix}$$

$$=\sum_K(2K+1)(-1)^{l_1+\Lambda-l_1'+l_2'+L'+K-\omega+\omega'-\Omega}$$

$$\times\begin{Bmatrix}l_1&\Lambda&l_1'\\l_2'&L'&K\end{Bmatrix}\begin{pmatrix}L'&l_1&K\\-\Omega&\omega&\Omega-\omega\end{pmatrix}$$

$$\times\begin{pmatrix}\Lambda&l_2'&K\\\omega'-\omega&\Omega-\omega'&\omega-\Omega\end{pmatrix}$$

defining $q=\omega'-\omega$; $t=\Omega-\omega'$, and taking into account the orthogonality properties

$$\sum_{qt}\begin{pmatrix}l_2'&\Lambda&l_2\\t&q&\omega-\Omega\end{pmatrix}\begin{pmatrix}l_2'&\Lambda&K\\t&q&\omega-\Omega\end{pmatrix}$$

$$=\delta_{Kl_2}(-1)^{l_2'+\Lambda+K}(2K+1)^{-1},$$

$$\sum_\omega\begin{pmatrix}l_1&l_2&L\\\omega&\Omega-\omega&-\Omega\end{pmatrix}\begin{pmatrix}L'&l_1&l_2\\-\Omega&\omega&\Omega-\omega\end{pmatrix}$$

$$=\delta_{LL'}(2L+1)^{-1}.$$

Equation (C3) finally transforms into Eq. (30). Note that this result coincides with that previously obtained by Edmonds,[24] p. 114, except the phase is $(-1)^{l_1-l_1'+L}$ instead of $(-1)^{l_1+l_2'+L}$.

[1] (a) W. Sharfin, K. E. Johnson, L. Wharton, and D. H. Levy, J. Chem. Phys. **71**, 1292 (1979); (b) J. E. Kenny, K. E. Johnson, W. Sharfin, and D. H. Levy, *ibid.* **72**, 1109 (1980); (c) K. E. Johnson, W. Sharfin, and D. H. Levy, *ibid.* **74**, 163 (1981).

[2] W. D. Sands, C. R. Bieler, and K. C. Janda, J. Chem. Phys. **95**, 729 (1991).

[3] S. R. Hair, J. I. Cline, C. R. Bieler, and K. C. Janda, J. Chem. Phys. **90**, 2935 (1989).

[4] C. R. Bieler, D. D. Edvard, and K. C. Janda, J. Chem. Phys. **94**, 7452 (1990).

[5] J. C. Drobits and M. I. Lester, J. Chem. Phys. **86**, 1662 (1987).

[6] M. Gutmann, D. M. Willberg, and A. H. Zewail, J. Chem. Phys. **97**, 8048 (1992).

[7] G. C. Schatz, V. Buch, M. A. Ratner, and R. B. Gerber, J. Chem. Phys. **79**, 1808 (1993).

[8] (a) N. Martín, G. Delgado-Barrio, P. Villarreal, P. Mareca, and S. Miret-Artés, J. Mol. Struct. **142**, 501 (1986); (b) G. Delgado-Barrio, P. Villarreal, A. Varadé, N. Martín, and A. García-Vela, in *Structure and Dynamics of Weakly Bound Molecular Complexes*, edited by A. Weber, NATO ASI C212 (Reidel, Dordrecht, 1987), p. 573.

[9] P. Villarreal, A. Varadé, and G. Delgado-Barrio, J. Chem. Phys. **90**, 2684 (1989).

[10] (a) P. Villarreal, S. Miret-Artés, O. Roncero, S. Serna, J. Campos-Martínez, and G. Delgado-Barrio, J. Chem. Phys. **93**, 4016 (1990); (b) P. Villarreal, S. Miret-Artés, J. Campos-Martínez, and G. Delgado-Barrio, in *Dynamics of Polyatomic van der Waals Complexes*, edited by N. Halberstadt and K. C. Janda, NATO ASI B227 (Plenum, New York, 1990), p. 517.

[11] A. García-Vela, P. Villarreal, and G. Delgado-Barrio, J. Chem. Phys. **92**, 496 (1990).

[12] (a) A. García-Vela, P. Villarreal, and G. Delgado-Barrio, J. Chem. Phys. **92**, 6504 (1990); (b) **94**, 7868 (1991).

[13] F. Le Quéré and S. K. Gray, J. Chem. Phys. **98**, 5396 (1993).

[14] Z. Bačić, M. Kennedy-Mandzink, and J. W. Moskowitz, J. Chem. Phys. **97**, 6472 (1992).

[15] M. Hernandez and N. Halberstadt, J. Chem. Phys. (submitted).

[16] G. Delgado-Barrio, A. García-Vela, J. Rubayo-Soneira, J. Campos-Martínez, S. Miret-Artés, O. Roncero, and P. Villarreal, in *Reaction Dynamics in Clusters and Condensed Phase*, edited by B. Pullman, J. Jortner, and R. D. Levine (Kluwer Academic, Dordrecht, 1994), p. 57.

[17] G. Delgado-Barrio, A. García-Vela, J. Rubayo-Soneira, and P. Villarreal (in preparation).

[18] L. L. Halcomb and D. J. Diestler, J. Chem. Phys. **84**, 3130 (1986).

[19] (a) G. Danby, J. Phys. B **16**, 3393 (1983); (b) G. Brocks, A van der Avoird, B. T. Sutcliffe, and J. Tennyson, Mol. Phys. **50**, 1025 (1983); (c) J. M. Hutson, J. A. Beswick, and N. Halberstadt, J. Chem. Phys. **90**, 1337 (1989); (d) D. C. Clary and P. J. Knowles, *ibid.* **93**, 6334 (1990); (e) A. R. Cooper and J. M. Hutson, *ibid.* **98**, 5337 (1993).

[20] (a) C. Lanczos, J. Res. Natl. Bur. Stand. **45**, 255 (1950); (b) C. Iung and C. Leforestier, J. Chem. Phys. **90**, 3198 (1989); (c) F. Le Quéré, Ph.D. thesis, Univeristé Paris-Sud, 1991; (d) G. Charron and T. Carrington, Jr., Mol.

Phys. **79**, 12 (1993); (e) A. McNichols and T. Carrington, Jr., Chem. Phys. Lett. **202**, 464 (1993).
[21] (a) G. A. Natanson, S. Ezra, G. Delgado-Barrio, and R. S. Berry, J. Chem. Phys. **81**, 3400 (1984); (b) **84**, 2035 (1986).
[22] (a) C. F. Curtiss, J. O. Hirschfelder, and F. T. Adler, J. Chem. Phys. **18**, 1638 (1950); (b) R. T Pack and J. O. Hirschfelder, *ibid.* **49**, 4009 (1968); (c) R. T Pack, *ibid.* **60**, 633 (1974); (d) G. C. Schatz and A. Kuppermann, *ibid.* **65**, 4642 (1976); (e) G. G. Balint-Kurti and M. Shapiro, Chem. Phys. **61**, 137 (1981).
[23] R. N. Zare, *Angular Momentum* (Wiley, New York, 1988).
[24] A. R. Edmonds, *Angular Momentum in Quantum Mechanics* (Princeton University, Princeton, 1957).
[25] J. A. Beswick and J. Jortner, Adv. Chem. Phys. **47**, 363 (1981).
[26] A. Messiah, *Mécanique Quantique* (Dunod, Paris, 1962), Vol. I, p. 145.
[27] Z. Bačić and J. C. Light, Annu. Rev. Phys. Chem. **40**, 469 (1989).
[28] W. H. Press, B. P. Flannery, S. A. Teukolsky, and W. T. Vetterling, *Numerical Recipes* (Cambridge University, Cambridge, 1986).
[29] M. Abramowitz and I. A. Stegun, *Handbook of Mathematical Functions* (Dover, New York, 1972), p. 887.
[30] G. Delgado-Barrio, in *Dynamical Processes in Molecular Physics*, edited by G. Delgado-Barrio (IOP, London, 1993).
[31] D. M. Willberg, M. Gutmann, J. J. Breen, and A. H. Zewail, J. Chem. Phys. **96**, 198 (1992).